⌘ *Author's Choice*

THE JOURNAL OF BIOLOGICAL CHEMISTRY VOL. 287, NO. 52, pp. 43995–44005, December 21, 2012

Cysteine 70 of Ankyrin-G Is *S*-Palmitoylated and Is Required for Function of Ankyrin-G in Membrane Domain Assembly[S]

Received for publication, September 6, 2012, and in revised form, October 29, 2012 Published, JBC Papers in Press, November 5, 2012, DOI 10.1074/jbc.M112.417501

Meng He[‡], **Paul Jenkins**[§¶], **and Vann Bennett**[§¶1]

From the [‡]*Department of Pharmacology and Cancer Biology, the* [§]*Howard Hughes Medical Institute, and the* [¶]*Departments of Biochemistry, Cell Biology, and Neurobiology, Duke University Medical Center, Durham, North Carolina 27710*

Background: Ankyrin-G targets to specialized membrane domains in multiple cell types.
Results: Ankyrin-G is *S*-palmitoylated at a conserved cysteine 70 located in the first loop of the ankyrin repeat solenoid.
Conclusion: Cysteine 70 is required for function of ankyrin-G in membrane domain assembly.
Significance: This finding provides new insights into how the ankyrin proteins exert their functions in formation and maintenance of membrane domains.

Ankyrin-G (AnkG) coordinates protein composition of diverse membrane domains, including epithelial lateral membranes and neuronal axon initial segments. However, how AnkG itself localizes to these membrane domains is not understood. We report that AnkG remains on the plasma membrane in Madin-Darby canine kidney (MDCK) cells grown in low calcium, although these cells lack apical-basal polarity and exhibit loss of plasma membrane association of AnkG partners, E-cadherin and β_2-spectrin. We subsequently demonstrate using mutagenesis and mass spectrometry that AnkG is *S*-palmitoylated exclusively at Cys-70, which is located in a loop of the first ankyrin repeat and is conserved in the vertebrate ankyrin family. Moreover, C70A mutation abolishes membrane association of 190-kDa AnkG in MDCK cells grown in low calcium. C70A 190-kDa AnkG fails to restore biogenesis of epithelial lateral membranes in MDCK cells depleted of endogenous AnkG. In addition, C70A 270-kDa AnkG fails to cluster at the axon initial segment of AnkG-depleted cultured hippocampal neurons and fails to recruit neurofascin as well as voltage-gated sodium channels. These effects of C70A mutation combined with evidence for its *S*-palmitoylation are consistent with a requirement of palmitoylation for targeting and function of AnkG in membrane domain biogenesis at epithelial lateral membranes and neuronal axon initial segments.

Ankyrins are a family of adaptors required for organization of functionally related proteins in diverse specialized membrane domains in vertebrate tissues (1). Neurons *in vivo* as well as in culture require AnkG[2] to fire action potentials and to populate the AIS with voltage-gated sodium channels, KCNQ2/3 channels, neurofascin, and β-4 spectrin (2–5). Interestingly, in the absence of AnkG, the AIS loses its axonal characteristics and acquires dendritic features (6, 7). Similarly, cultured epithelial cells require AnkG to form a new lateral membrane following cell division (8). AnkG is also localized to rod outer segments, where it interacts with the CNG-β subunit of the cyclic nucleotide-gated channel (9), and to costameres in skeletal muscle, where it associates with dystrophin and dystroglycan (10). Additionally, AnkG targets to cardiac intercalated discs, where it interacts with sodium channel signaling complexes (11–13).

It is unclear how AnkG itself localizes to specialized membrane domains. Multiple AnkG domains are required to direct AnkG to the AIS of dorsal root ganglion neurons and lateral membranes of cultured epithelial cells (8, 14). Elimination of the AnkG binding partners, β_4-spectrin or neurofascin, does not prevent localization of AnkG at the AIS (5, 15, 16). Recent work has shown that ankyrin-B is critical to confine AnkG to the AIS, although the mechanism for axonal localization remains unclear (17). In epithelial cells, a DAR999AAA mutant AnkG, which specifically loses interaction with β_2-spectrin, still efficiently localizes to the lateral membrane, although this mutant AnkG lacks activity in membrane biogenesis (18). Therefore, additional features mediated by interactions with unidentified proteins or membrane phospholipids may contribute to targeting of AnkG to specialized membrane domains.

Covalent modification of proteins with lipids can contribute to micropatterning of plasma membranes (19). Interestingly, ankyrin-R purified from erythrocyte membranes exhibited hydrophobicity intermediate between a cytosolic protein and an integral protein (20). Moreover, ankyrin-R is palmitoylated in a reversible fashion (21). In the present study, we report that AnkG is *S*-palmitoylated at a cysteine conserved among all three ankyrin family members and located in their membrane-binding domains. We also find that the same cysteine, possibly due to its *S*-palmitoylation, is required for targeting as well as the biological functions of AnkG in epithelial cells and neurons.

EXPERIMENTAL PROCEDURES

Reagents, Plasmids, and Antibodies—*N*-Ethylmaleimide and hydroxylamine were from Sigma; EZ-Linker Biotin-BMCC was from Thermo; activated thiol-Sepharose 4B was from GE

⌘ *Author's Choice*—Final version full access.
[S] This article contains supplemental Figs. 1 and 2.
[1] To whom correspondence should be addressed: Howard Hughes Medical Institute and Dept. of Biochemistry, Duke University Medical Center, Durham, NC 27710. Tel.: 919-684-3538; Fax: 919-684-3025; E-mail: vann.bennett@duke.edu.
[2] The abbreviations used are: AnkG, ankyrin-G; AIS, axon initial segment; MDCK, Madin-Darby canine kidney cells; ZO-1, zonula occludens-1; FRAP, fluorescence recovery after photobleaching; ANOVA, analysis of variance; DAR999AAA, D999A/A1000A/R1001A; BMCC i, 1-Biotinamido-4-[4′-(maleimidomethyl)cyclohexanecarboxamido]butane.

Healthcare; Dynabeads with protein-G and the Lipofectamine 2000 transfection reagent were from Invitrogen; the QuikChange II XL site-directed mutagenesis kit was from Agilent Technologies; and palmitic acid, 9,10-^{3}H-labeled, was from PerkinElmer Life Sciences. Rat wild-type 190-kDa AnkG cDNA was described previously (8). Rabbit polyclonal antibody targeting the C-terminal domain of AnkG and rabbit polyclonal antibody against β_2-spectrin were described previously (18); mouse monoclonal antibodies against human E-cadherin and ZO-1 were from Invitrogen; mouse monoclonal anti-sodium channel pan-antibody was from Sigma; and rabbit polyclonal antibody against biotin was from Abcam.

MDCK Stable Cell Lines—The ViraPower Lentiviral Expression System based on the pLenti6/V5-DEST gateway vector from Invitrogen was used to generate stable MDCK cell lines expressing wild-type or C70A AnkG-GFP. For lentivirus generation, 293T cells were grown in Dulbecco's modified Eagle's medium (DMEM) supplemented with 10% fetal bovine serum. 15 million cells were plated in 100-mm dishes and transfected the next day with 16 μg of cDNA (4 μg of pMDLg/pRRE, 4 μg of pRSV-Rev, 4 μg of pMD2.G, and 4 μg of transfer plasmid) using Lipofectamine 2000 following the manufacturer's protocol. 48 h later, 25 ml of culture medium were collected and centrifuged at 25,000 rpm for 2 h to collect the virus. Half a million MDCK cells were plated in a 6-well plate and infected with virus for 16 h. Blasticidin S was used to select infected cells and establish a stable cell line.

Calcium Switch Assay—MDCK cells were maintained in DMEM supplemented with 10% FBS until they formed a polarized monolayer. Cells were then trypsinized, and 2×10^6 cells were plated on 14-mm coverslip inserts of MatTek plates in calcium-free minimum essential medium supplemented with 5% dialyzed low calcium FBS. 16 h later, cells were washed with PBS to remove unattached cells and then fed with normal growth medium. Cells were fixed and processed for immunofluorescence to visualize protein localization at multiple time points.

Membrane Recruitment Assay—This assay was reported previously (14). Briefly described, 1×10^5 HEK293 cells were plated in 14-mm insert, collagen-coated MatTek plates. The next day, cells were co-transfected with 100 ng of HA-tagged neurofascin or E-cadherin cDNA and 80 ng of GFP-tagged 190-kDa AnkG cDNA using Lipofectamine 2000. 24 h later, cells were fixed and processed for immunofluorescence as described below.

Biotin Switch Assay—The biotin switch assay was described previously for testing protein *S*-acylation (22). Because endogenous AnkG is resistant to Triton X-100 extraction, we developed a protocol for solubilizing AnkG from MDCK cells in a state compatible with immunoprecipitation. A polarized MDCK monolayer in a 150-mm dish was washed and suspended in ice-cold PBS buffer with protease inhibitors; cells were then collected by centrifugation at $1000 \times g$ for 5 min. The cell pellet was homogenized in lysis buffer (10 mM sodium phosphate, 2 mM NaEDTA, 0.32 M sucrose, 50 mM *N*-ethylmaleimide, and protease inhibitors (10 μg/ml 4-(2-aminoethyl)-benzenesulfonyl fluoride, 30 μg/ml benzamidine, 10 μg/ml pepstatin, and 10 μg/ml leupeptin), pH 7.4) using a 27-gauge needle and incubated at 4 °C for 6 h to preblock free sulfhydryl groups. SDS was then added to the lysates at a final concentration of 1% (w/v) and mixed well immediately. Lysates were sonicated for 30 s on ice followed by centrifugation at $100,000 \times g$ for 30 min. Triton X-100 was then added to a final concentration of 1% (v/v) and then mixed well and incubated on ice for 30 min followed by rotation at 4 °C for another 30 min to quench SDS. 60 μl of Dynabeads preloaded with 10 μg of AnkG antibody were then incubated with the lysates overnight, rotating at 4 °C. The beads were washed three times with cold wash buffer (10 mM sodium phosphate, 2 mM NaEDTA, and protease inhibitors, pH 7.4) and then incubated with hydrolysis-labeling buffer (1 M hydroxylamine, 80 μM Biotin-BMCC, 10 mM sodium phosphate, 2 mM NaEDTA, and protease inhibitors, pH 7. As a control, 1 M Tris-HCl was substituted for hydroxylamine) at room temperature for 2 h. Beads were then washed three times with wash buffer and incubated with 5× loading buffer (5% SDS, 20% sucrose, 40 mM Tris-HCl, 150 mM NaCl, 2 mM NaEDTA, 200 mM DTT with bromphenol blue) at 70 °C for 15 min to elute proteins. Samples were analyzed by SDS-PAGE and Western blotting. A biotin antibody was used to detect *S*-acylation.

Mass Spectrometry—HEK293 cells transfected with WT AnkG-GFP were homogenized in lysis buffer (10 mM sodium phosphate, 2 mM NaEDTA, 0.32 M sucrose, 50 mM *N*-ethylmaleimide, and protease inhibitors (10 μg/ml 4-(2-aminoethyl)-benzenesulfonyl fluoride, 30 μg/ml benzamidine, 10 μg/ml pepstatin, and 10 μg/ml leupeptin), pH 7.4) and incubated at 4 °C for 6 h to preblock free sulfhydryl groups. Triton X-100 was then added at 1% final concentration, and lysates were sonicated for 20 s. Dynabeads preloaded with GFP antibody (GFP antibody was blocked with *N*-ethylmaleimide) were then added to immunoprecipitate AnkG-GFP overnight. The following day, the beads were washed three times and incubated with elution buffer (1% SDS, 10 mM sodium phosphate, 2 mM NaEDTA, 0.32 M sucrose) at 50 °C for 5 min to selectively release AnkG-GFP. Eluted samples were divided into two equal portions: one treated with 1 M hydroxylamine and the other with 1 M Tris-HCl (as a control) at neutral pH with the presence of activated thiol-Sepharose 4B. After a 2-h incubation at 24 °C, Sepharose beads were washed with 20 mM ammonium bicarbonate three times and digested in 0.1% Rapigest reagent. After trypsin digestion, the beads were incubated with 20 mM DTT at 24 °C for 45 min to elute cysteine-containing peptides. Eluted samples were alkylated with 40 mM iodoacetamide and analyzed by LC-MS/MS.

[^{3}H]Palmitic Acid Labeling—8×10^6 stable MDCK cells of WT or C70A AnkG-GFP were plated on 100-mm dishes and grown in 37 °C, 5% CO_2 overnight. The next day, cells were rinsed with PBS buffer and incubated with 5 ml of serum-free medium for 4 h, and then the medium was replaced with 5 ml of fresh DMEM containing 100 μCi/ml [^{3}H]palmitic acid. Following a 4-h incubation, AnkG-GFP was immunoisolated using the protocol described previously and divided into two equal portions, one treated with 1 M hydroxylamine and the other treated with 1 M Tris-HCl at room temperature for 2 h. Proteins were then eluted, separated by SDS-PAGE, and transferred to a nitrocellulose membrane, which was then exposed for 6 weeks at −80 °C to detect tritium radioactivity.

Immunostaining and Fluorescence Recovery after Photobleaching—MDCK cells on MatTek plates were first washed with cold PBS and fixed with 4% paraformaldehyde at room temperature for 15 min, and then cells were permeabilized with 0.2% Triton X-100 at room temperature for 10 min. Following a 30-min blocking in PBS buffer containing 2% bovine serum albumin, cells were incubated with primary antibody at 4 °C overnight. Cells were next washed with PBS buffer three times and then incubated with fluorescence-conjugated secondary antibodies (AlexaFluor 488, 568, or 663, Molecular Probes) at room temperature for 2 h. Fluorescent antibody labeling was visualized using a Zeiss LSM 510 laser-scanning microscope. Images from Figs. 1 and 7 were collected using the ×63, numerical aperture 1.4 objective lens, and *xz* planes were reconstructed from *z* stacks with optical sections of 0.5 μm. Images from Figs. 4 and 6 were collected using a ×100, numerical aperture 1.45 objective lens, and *xz* planes were reconstructed from *z* stacks with optical sections of 0.37 μm. Volocity three-dimensional image analysis software was used to measure the fluorescence intensity of plasma membrane and cytoplasm. Data were analyzed using GraphPad Prism version 5. For fluorescence recovery after photobleaching (FRAP) measurements, MDCK cells grown on MatTek plates were transfected with 300 ng of WT, C70A, DAR999AAA, or C70A/DAR999AAA double mutation AnkG-GFP plasmids. 24 h later, cells were analyzed using a Zeiss LSM 780 laser-scanning confocal system. The selected membrane region was bleached for 5 s, and the fluorescence recovery was monitored for the following 500 s. An unbleached region was also monitored during the measurements and was used to normalize the FRAP data. GraphPad Prism version 5 was used to analyze the data by fitting them to the one-phase association equation, $y = y_0 + Ae^{-}k \times t$.

Doxycycline-inducible shRNA Cell Lines and Rescue Experiments—The Tet-pLKO-puro vector was originally obtained from Addgene (Plasmid 21915). We replaced the puromycin resistance gene with mCherry to allow isolation of transfected cells by fluorescence activated cell sorting (FACS), whereas the internal ribosome entry site region was replaced with the foot and mouth disease virus 2A peptide (GSGATNFSLLKQAGDVEENPGP) to facilitate higher expression levels of mCherry. Oligonucleotides encoding an shRNA hairpin targeting canine AnkG in the ankyrin repeat domain (gctagaagtagctaatctcct) were cloned into Tet-pLKO-2A-mCherry, with hairpin targeting the luciferase gene (ggagatcgaatcttaatgtgc) as a negative control. Lentivirus was generated using the second generation packaging system from Addgene (psPAX2 and pMD2.G) following the recommended protocol. Two days after MDCK cells were infected, cells were trypsinized and fractionated by FACS to establish a stable cell line. To evaluate AnkG knockdown efficiency, stable cells were induced by 5 μg/ml doxycycline for 24 and 48 h. Total RNA was extracted following standard protocol and applied for real-time quantitative PCR using Power SYBR Green Master Mix from Invitrogen. For rescue experiments, cells were preinduced for 12 h using 5 μg/ml doxycycline and replated on 14-mm insert MatTek plates with the presence of doxycycline at a density of 1600/mm^2. 6 h later, cells were transfected with 80 ng of WT or C70A AnkG-GFP using Lipofectamine 2000. Cells were supplemented with fresh medium 4 h post-transfection and fixed for immunofluorescence after 36 h.

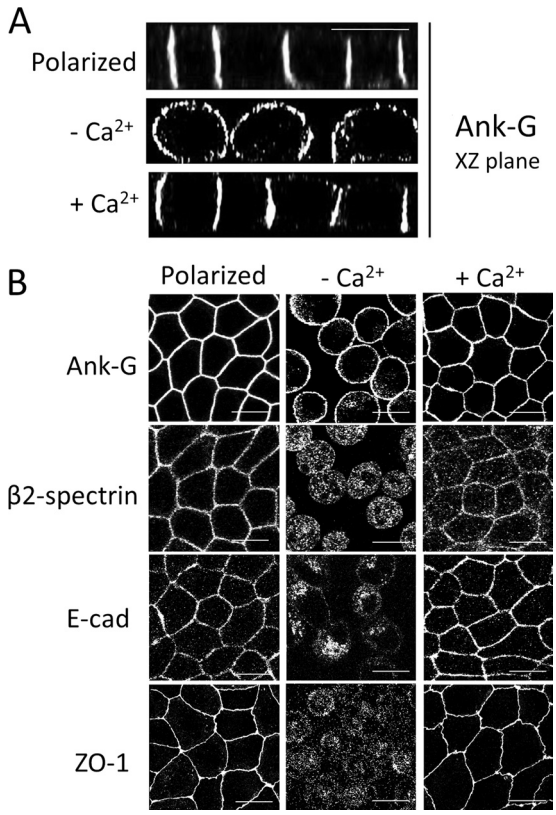

FIGURE 1. **AnkG remains membrane-associated in MDCK cells following calcium switch.** *A* and *B*, fully polarized MDCK cells (polarized) were trypsinized and replated in Ca^{2+}-free medium with 5% FBS overnight to reach a steady state. Cells were then either fixed ($-Ca^{2+}$) or allowed 24 h to recover in normal growth medium ($+Ca^{2+}$) and then fixed and processed for immunofluorescence to stain against AnkG, β_2-spectrin, E-cadherin, and ZO-1. *A*, the *xz* planes showing AnkG staining in MDCK cells following calcium switch described above. *B*, the *xy* planes showing immunostaining of AnkG, β_2-spectrin, E-cadherin (*E-cad*), and ZO-1 (a marker of tight junction) in MDCK cells following calcium switch. *Scale bars*, 10 μm. Images are representative of at least three independent repeated experiments.

Hippocampal Neuronal Cultures—Hippocampi were dissected from neonatal C57bl/6 mice (P0-P1) and incubated in 2 mg/ml papain in Hibernate A with 100 μg/ml DNase at 37 °C for 20 min. Hippocampi were washed twice in plating medium (Neurobasal A plus 2% B-27 supplement, 2 mM Glutamax, and 10% horse serum) and triturated first with a P200 pipette tip and then with a fire-polished Pasteur pipette until dissociated. Cells were resuspended in plating medium and plated in poly-L-lysine-coated MatTek plates for 3–4 h. Medium was gently aspirated and replaced with growth medium (Neurobasal A plus 2% B-27 supplement and 2 mM Glutamax) for 4–5 days. Transfections were carried out with Lipofectamine 2000. In one tube, 1 μg of total cDNA was mixed with 100 μl of Neurobasal A, and in a second tube, 3 μl of Lipofectamine 2000 was mixed with 100 μl of Neurobasal A. After 15 min, tubes were mixed. Growth medium was removed from neurons and set aside, and transfection mixture was added to cells. After 1 h at 37 °C, the transfection mix was aspirated, and cells were fed with the original growth medium supplemented with 5 μM cytosine arabinoside. After 48 h (7 days in vitro), cells were fixed with 4% paraformaldehyde for 15 min at room temperature and ice-cold

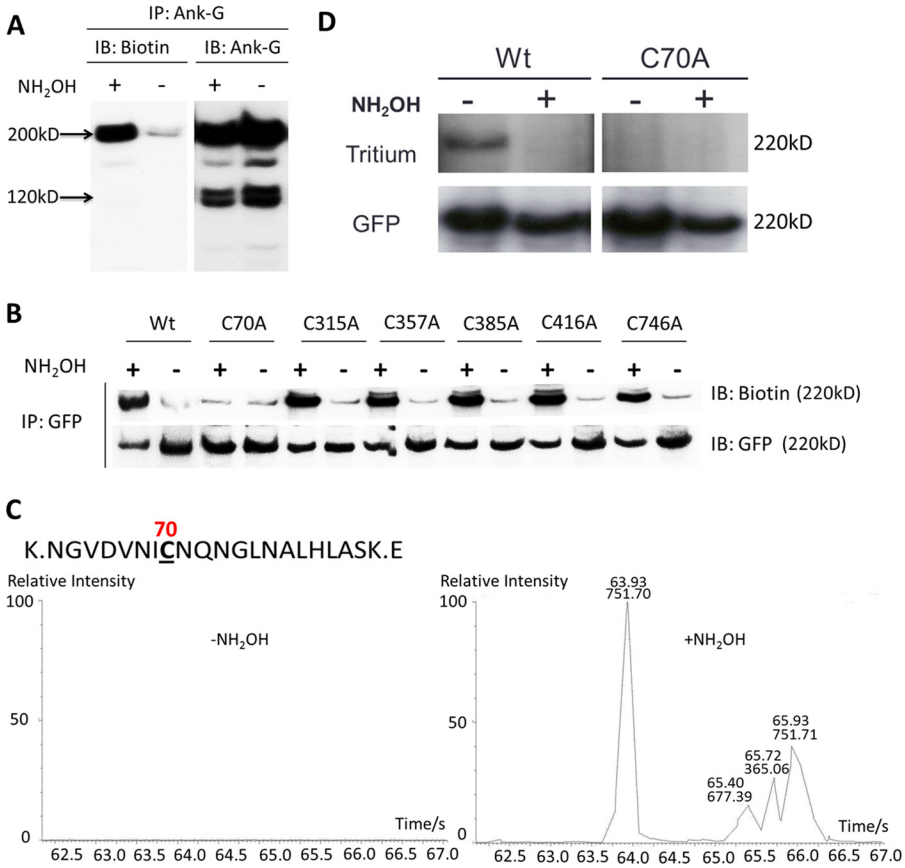

FIGURE 2. **AnkG is *S*-palmitoylated at cysteine 70.** *A*, endogenous AnkG was immunoprecipitated (*IP*) from MDCK cell lysates and processed for the biotin switch assay (see "Experimental Procedures") to detect protein *S*-acylation. Four major AnkG polypeptides are detected in MDCK cells using an antibody against the C-terminal region. The blot (*IB*) shows that only the ~200-kDa isoform, which has ankyrin repeats, is *S*-acylated (blots are representative of three independent experiments). *B*, GFP-tagged wild-type AnkG and cysteine-to-alanine mutants (C70A, C315A, C357A, C385A, C416A, and C746A) were transfected into HEK293 cells and processed for the biotin switch assay. The blot shows that C70A completely abolishes AnkG *S*-acylation. (Blots are representative of two independent experiments.) *C*, HEK293 cells transfected with AnkG-GFP were lysed and blocked with *N*-ethylmaleimide. Following immunoisolation, AnkG was incubated with activated thiol-Sepharose 4B in the presence of hydroxylamine (or Tris buffer as a negative control). Sepharose samples were then digested and eluted after extensive washes. Eluted samples were analyzed using LC/MS, which identified an *S*-acylated AnkG peptide KNGVDVNICNQNGLNALHLASKE containing cysteine 70 (for details, see "Experimental Procedures"). *C*, a mass chromatogram of the selected AnkG peptide. *D*, stable MDCK cell lines of WT or C70A AnkG-GFP were labeled with 100 μCi/ml [^{3}H]palmitic acids. AnkG was then immunoprecipitated and analyzed by SDS-PAGE. The blot shows that radioactive palmitic acids can be incorporated into WT AnkG but not C70A in a hydroxylamine-sensitive way (the experiment was performed once).

methanol for 7 min at −20 °C and processed for immunostaining. For quantification, confocal *z* stack images were collapsed, and the mean fluorescence intensities from dendrites and the first 60 μm of axons were measured using ImageJ software. The intensity ratios of axon to dendrite were quantified and analyzed using GraphPad Prism version 6.

RESULTS

AnkG Remains on the Plasma Membrane in MDCK Cells Grown in Low Calcium—MDCK cells are well known to require extracellular calcium to maintain transepithelial resistance and apical-basal polarity (23). Adherens junction proteins (E-cadherin), tight junction proteins (zonula occludens-1 (ZO-1)), desmosomal proteins (desmoplakin), and components of the spectrin-based membrane skeleton all depend on extracellular calcium for their localization at lateral membrane domains of MDCK cells (24–27). Here we determined the effects of low calcium on localization of AnkG and its binding partners, E-cadherin and β_2-spectrin. MDCK cells grown in low calcium medium lacked cell-cell contacts and exhibited a spherical morphology (Fig. 1, *A* and *B*). As reported previously, E-cadherin is intracellular in unpolarized MDCK cells and accumulates at the region of cell-cell contact only after the addition of calcium (26, 28). β_2-spectrin also exhibits a similar pattern and associates with the plasma membrane only following the addition of calcium (29) (Fig. 1*B*). However, we were surprised to observe a substantial fraction of AnkG that remained associated with the plasma membrane in low calcium and in the absence of cell-cell contacts (Fig. 1, *A* and *B*). Following elevation of calcium, AnkG reorganized and concentrated at the lateral membrane to achieve polarized localization (Fig. 1, *A* and *B*). As far as we are aware, AnkG is the only lateral membrane-associated protein identified so far that remains on the plasma membrane in MDCK cells following depletion of calcium.

AnkG Is S-Palmitoylated at Cysteine 70—The finding that AnkG associates with the plasma membrane in non-polarized MDCK cells in the absence of β_2-spectrin and E-cadherin suggested the possibility of a protein-independent mode of membrane interaction though lipidation. *S*-Acylation plays critical roles in membrane interactions, intracellular sorting, protein stability, and signaling (30). It is pertinent in this regard that

ankyrin-R was reported to undergo palmitoylation, although an amino acid site(s) was not identified (31). We therefore explored possible *S*-acylation of AnkG in MDCK cells using a biotin switch assay (22). In this assay, proteins with free sulfhydryl groups were first blocked by *N*-ethylmaleimide and then treated with hydroxylamine (or Tris as a negative control), which selectively cleaves thioester bonds and releases new sulfhydryl groups for labeling using sulfhydryl-reactive biotinylation reagent (BMCC-Biotin). We found that 210-kDa AnkG was *S*-acylated in MDCK cells (Fig. 2*A*). Two smaller AnkG polypeptides with molecular masses of 100 and 120 kDa, which lack ankyrin repeats (32), were not *S*-acylated (Fig. 2*A*).

We next identified the principal *S*-acylated cysteine(s) of AnkG by mutagenesis. Considering that only full-length AnkG is *S*-acylated, we created cysteine to alanine mutants of all of the cysteines in the membrane-binding domain (C70A, C315A, C357A, C385A, C416A, and C746A). These AnkG mutants were expressed in HEK293 cells and processed for the biotin switch assay to detect protein *S*-acylation. As shown in Fig. 2*B*, WT AnkG as well as C315A, C357A, C385A, C416A, and C746A mutants are all *S*-acylated in HEK293 cells, demonstrating that this modification is not limited to epithelial cells. However, the C70A mutation completely abolished the specific biotin signal (Fig. 2*B*).

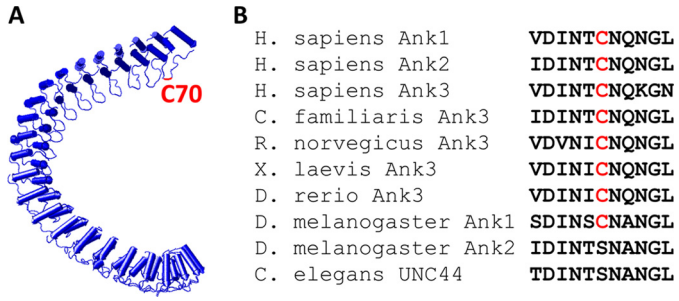

FIGURE 3. **The conservation of cysteine 70 and its position in the predicted ankyrin repeat structure.** *A*, a predicted structure of ankyrin repeats shows that cysteine 70 (*C70*) locates in the loop connecting the first two repeats, *highlighted* in *red*. *B*, cysteine 70 is conserved among three human ankyrin members and also conserved in AnkG across different species.

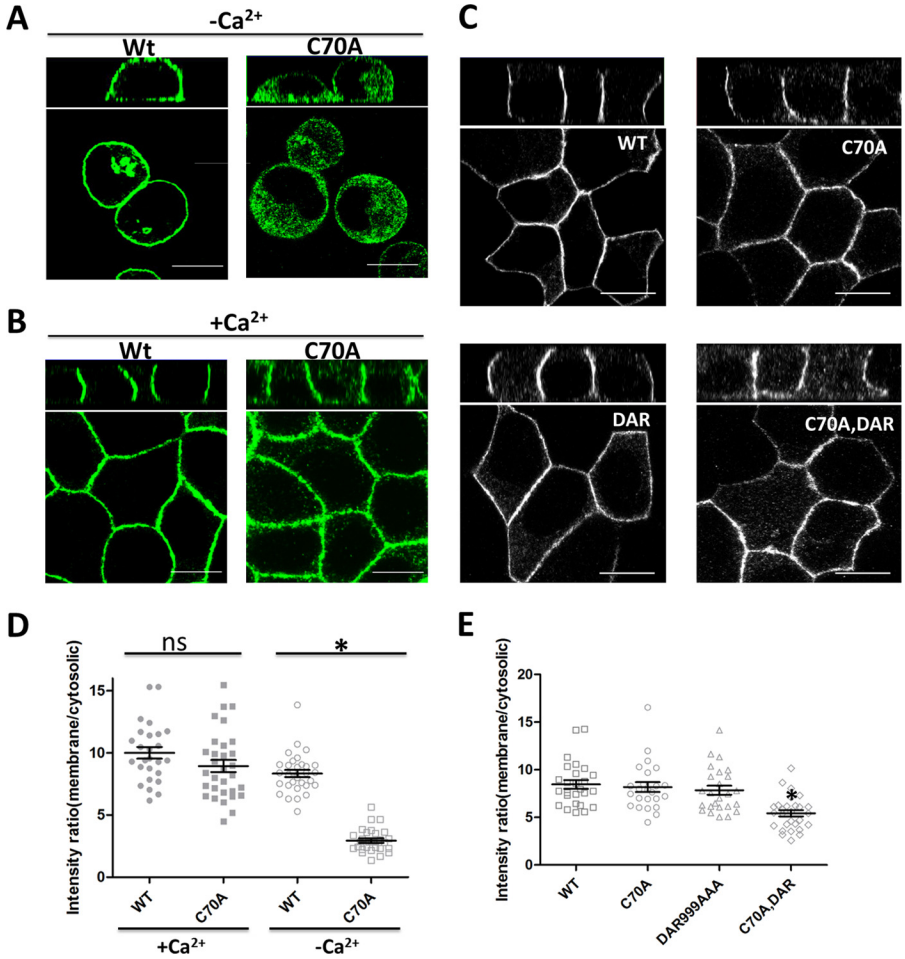

FIGURE 4. **C70A mutation prevents AnkG retention in MDCK cells grown in low calcium.** *A*, stable MDCK cells expressing WT or C70A AnkG-GFP were grown in low calcium medium overnight and then fixed and immunostained against GFP. *B*, stable MDCK cells expressing WT or C70A AnkG-GFP were grown in normal medium to reach a polarized monolayer and then fixed and immunostained against GFP. *C*, 60 ng of WT, C70A, DAR999AAA (*DAR*), and DAR999AAA/C70A double mutant (*C70A, DAR*) AnkG-GFP cDNA were transfected into MDCK cells in 14-mm MatTek plates. Cells were then fixed and immunostained against GFP 24 h post-transfection (*green channel* in *grayscale*). *Scale bars*, 10 μm for *A–C*. *D*, quantitative results of the fluorescence intensity ratio of plasma membrane *versus* cytoplasmic staining in AnkG stable MDCK cell lines. Data were compared using one-way ANOVA followed by a Tukey post hoc test ($p < 0.001$ for ANOVA, $n = 26–31$ from two independent experiments). *, $p < 0.05$; *ns*, not significant. *E*, quantitative results of the fluorescence intensity ratio of plasma membrane *versus* cytoplasmic staining of WT, C70A, DAR999AAA (*DAR*), and DAR999AAA/C70A double mutant (*C70A, DAR*) transfected into MDCK cells. Data were compared using one-way ANOVA followed by a Tukey post hoc test ($p < 0.001$ for ANOVA, $n = 26–28$ from three independent experiments). *, $p < 0.05$. *Error bars*, S.E.

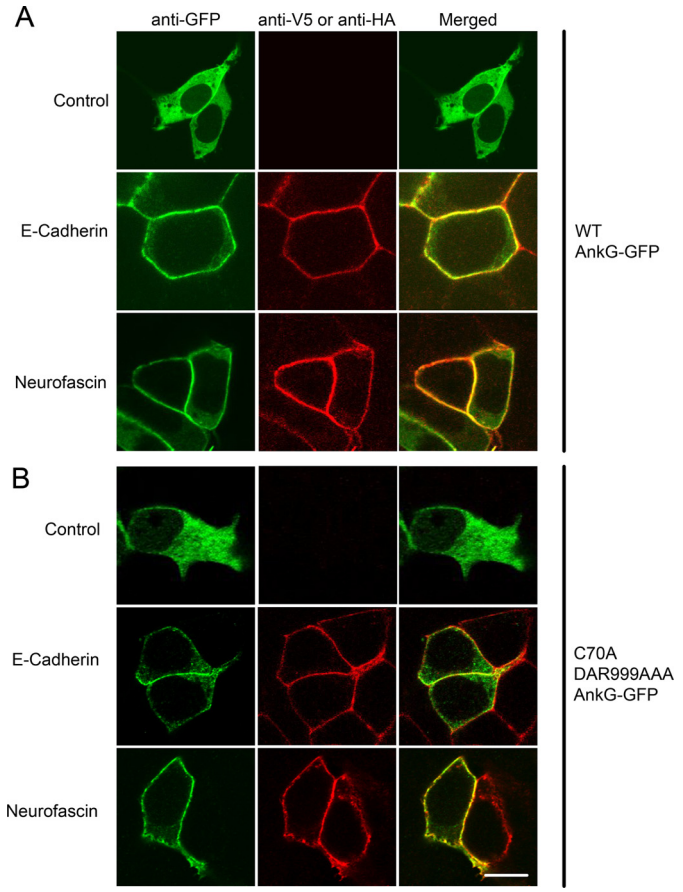

FIGURE 5. **Cys-70 mutation does not affect AnkG interactions with E-cadherin or neurofascin.** The membrane recruitment assay was used to monitor AnkG interactions with the interacting partners, E-cadherin and neurofascin. 80 ng of WT AnkG-GFP (*A*) or C70A/DAR999AAA AnkG-GFP (*B*) was transfected into HEK293 cells with or without (*Control*) 100 ng of binding partner (V5-E-cadherin or HA-neurofascin). Cells were then fixed and double-stained with anti-HA or -V5 (*red*) and anti-GFP (*green*) antibodies (*scale bar*, 10 μm).

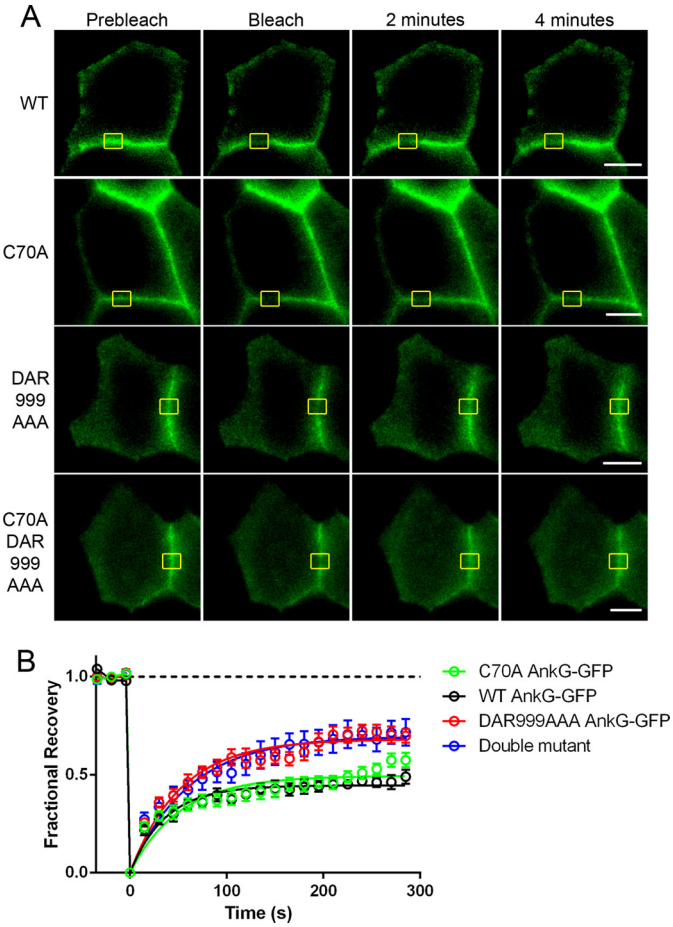

FIGURE 6. **Effects of C70A mutation on AnkG dynamics at the lateral membrane.** *A*, 300 ng of WT, C70A, DAR999AAA, and C70A/DAR999AAA double mutant AnkG-GFP were transfected into MDCK cells plated in 14-mm MatTek plates. FRAP was performed using an LSM780 laser-scanning confocal microscope. The representative graphs show the fluorescence recovery within 5 min; *yellow boxes* indicate the regions bleached. *B*, quantitative results of $n = 10$ repetitive measurements. The normalized fluorescence intensities were plotted against time and regressed against the one-phase exponential equation, $y = y_0 + Ae^{-}k \times t$, using GraphPad Prism version 5 (*scale bar*, 10 μm). *Error bars*, S.E.

In separate experiments, we employed mass spectrometry as an independent approach to identify *S*-acylated peptides in AnkG. We isolated *S*-acylated AnkG by first blocking free SH groups in cells with *N*-ethylmaleimide, followed by removal of thioester groups with hydroxylamine as described above for the biotin switch assay. We then isolated *S*-acylated AnkG using activated thiol-Sepharose 4B (33). Following proteolysis, the *S*-acylated peptide(s) were eluted with dithiothreitol and then alkylated with iodoacetamide. Using liquid chromatography and mass spectrometry, we identified a single AnkG peptide, KNGVDVNICNQNGLNALHLASKE, which contains Cys-70, confirming that cysteine 70 was indeed *S*-acylated (Fig. 2*C*). Fig. 2*C* shows the selected ion chromatograms of the identified peptide from both control ($-NH_2OH$) and experimental ($+NH_2OH$) samples.

Protein *S*-acylation can occur by modification with multiple fatty acids (34). We therefore next tested whether AnkG *S*-acylation is mediated by palmitic acid. MDCK stable cells expressing WT or C70A AnkG-GFP were metabolically labeled with tritiated palmitic acid, followed by immunoisolation of AnkG-GFP. We found that palmitic acid was incorporated into wild type AnkG-GFP, but not the C70A mutant, and that palmitoylation was reversed by hydroxylamine but not by Tris-HCl (Fig. 2*D*). These results provide direct evidence that palmitic acid is coupled to cysteine 70 of AnkG through a thioester bond.

Cys-70 is located in a loop of the first ankyrin repeat in the membrane-binding domain of AnkG (Fig. 3*A*). Interestingly, Cys-70 is conserved among all three human ankyrin members as well as all vertebrate ankyrins. Interestingly, *Drosophila* ankyrin isoform 1 also has a cysteine at the comparable position, whereas the single *Caenorhabditis elegans* ankyrin and *Drosophila* ankyrin isoform 2 both contain a serine instead of cysteine (Fig. 3*B*). These results suggest strong evolutionary pressure and a conserved function(s) shared between the three vertebrate ankyrins and one of the *Drosophila* ankyrin genes.

AnkG Requires Cys-70 for Membrane Association in MDCK under Low Calcium Conditions—We next explored the role of cysteine 70 in targeting of AnkG to the plasma membrane of MDCK cells grown in low calcium, where other known ankyrin-G protein partners are absent (Fig. 1). We evaluated the localization of WT or C70A AnkG-GFP in MDCK cells grown in low calcium medium by measuring the fluorescence intensity ratios of membrane to cytosolic staining. A majority of

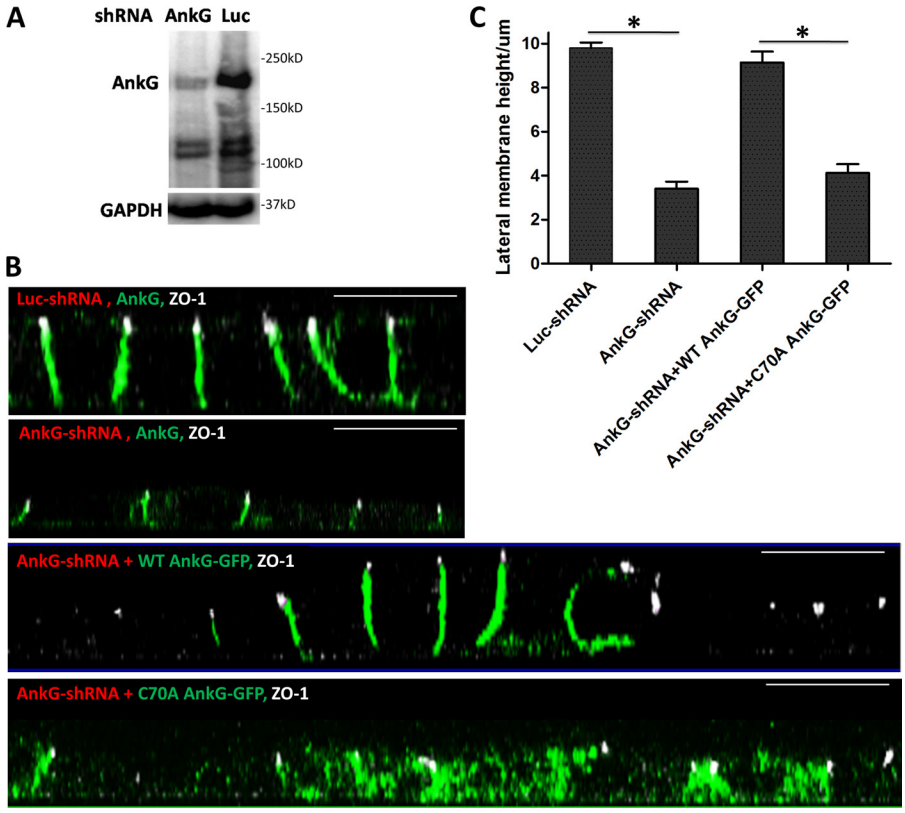

FIGURE 7. **C70A mutation abolishes AnkG function in lateral membrane biosynthesis.** *A*, doxycycline-inducible AnkG shRNA MDCK cell line was generated using an engineered Tet-pLKO-mCherry vector. Two days of doxycycline induction could selectively knock down 90% of ~200-kDa AnkG. (Blot is representative of at least three independent experiments). *B*, XZ planes of lateral membrane under different conditions (*green*, AnkG; *white*, ZO-1, *scale bar*, 10 μm). AnkG knockdown cells show a defect in lateral membrane height compared with luciferase-shRNA cells. WT AnkG, but not the C70A mutant, is able to restore the height of lateral membrane. *C*, quantitative results of the height of lateral membranes. The height was defined as the distance between the bottom of ZO-1 staining and the end of the lateral membrane. Mean lateral membrane height was 9.8 $\pm$ 0.3 μm for luciferase shRNA, 3.4 $\pm$ 0.4 μm for AnkG shRNA, 9.1 $\pm$ 0.6 μm for WT-AnkG rescue, and 4.1 $\pm$ 0.5 μm for rescue with C70A AnkG-GFP. Conditions were compared using one-way ANOVA followed by a Tukey post hoc test ($p < 0.001$ for ANOVA, $n = 24$–30/condition). *, $p < 0.05$. *Error bars*, S.E.

WT AnkG-GFP remains on the plasma membrane, as observed with native AnkG (Fig. 1*A*). In contrast, the C70A mutant was mainly distributed in the cytoplasm (Fig. 4, *A* and *D*). WT and C70A AnkG-GFP show average intensity ratios between plasma membrane and cytoplasm of 8.3 $\pm$ 0.3 and 2.7 $\pm$ 0.2, respectively ($p < 0.001$). This observation indicates that Cys-70 is required for targeting AnkG to the plasma membrane in the absence of E-cadherin and β_2-spectrin. Interestingly, WT AnkG-GFP also associates with internal structures that are currently uncharacterized.

One interpretation of loss of C70A AnkG association with plasma membranes of unpolarized MDCK cells (Fig. 4*A*) is that Cys-70 may be required for stable folding or protein-protein interactions. We therefore examined membrane localization of C70A AnkG in polarized MDCK cells, which display normal localization of AnkG binding partners (Fig. 1*B*). In contrast to unpolarized MDCK cells, WT and C70A AnkG associate equivalently with the lateral membrane in polarized MDCK cells (Fig. 4, *B* and *D*; WT and C70A AnkG-GFP show indistinguishable average intensity ratios between plasma membrane and cytoplasm of 10 $\pm$ 0.5 and 8.9 $\pm$ 0.5, respectively; $p = 0.1248$).

In order to compare the effects of C70A mutation with a loss of spectrin binding mutation, we utilized a DAR999AAA mutant AnkG that lacks spectrin-binding activity (18). We compared the plasma membrane targeting of WT, C70A, DAR999AAA, and C70A/DAR999AAA double-mutated AnkG expressed by transient transfection of MDCK cells. Both the DAR999AAA mutant and C70A/DAR999AAA double AnkG mutant exhibited plasma membrane localization. However, more of the double mutant remained cytosolic than with either mutation alone (Fig. 4, *C* and *E*). WT, C70A, DAR999AAA, and C70A/DAR999AAA double-mutated AnkG show average intensity ratios between plasma membrane and cytoplasm of 8.5 $\pm$ 0.4, 8.1 $\pm$ 0.5, 7.8 $\pm$ 0.5, and 5.4 $\pm$ 0.3, respectively ($p <$ 0.001).

To evaluate the possibility that C70A mutation interferes with AnkG binding to known membrane-spanning proteins, we directly evaluated the ability of C70A mutant AnkG-GFP to interact with E-cadherin and neurofascin using a membrane recruitment assay in 293 cells. This assay takes advantages of the fact that WT AnkG, when expressed at high levels, exists in the cytoplasm but can be recruited to the plasma membrane if co-expressed with a membrane partner. Detailed information on this assay can be found in previous publications (14, 35). WT and C70A/DAR999AAA double mutant AnkG both were cytosolic when overexpressed in 293 cells but were equivalently recruited to the plasma membrane when co-transfected with either E-cadherin or neurofascin (Fig. 5). C70A mutation thus has no effect on association of AnkG with at least two of its known protein partners. These results taken together are con-

sistent with a role of palmitoylation of Cys-70 in membrane targeting of ankyrin-G to the membrane of unpolarized MDCK cells (Fig. 4*A*).

Effect of C70A and DAR999AAA Mutations on AnkG Membrane Dynamics—It is known that palmitoylation can alter membrane protein dynamics and intracellular trafficking (36). Here, we used FRAP to examine whether C70A and DAR999AAA mutations affect mobility of GFP-tagged 190-kDa AnkG within the lateral membrane of polarized MDCK cells. WT AnkG exhibited rapid recovery to about 40% of its prebleach intensity in the first 100 s following photobleaching. However, WT AnkG exhibited little further recovery in the remaining 400 s, demonstrating a substantial immobile fraction of around 60% in the time scale of these measurements. In order

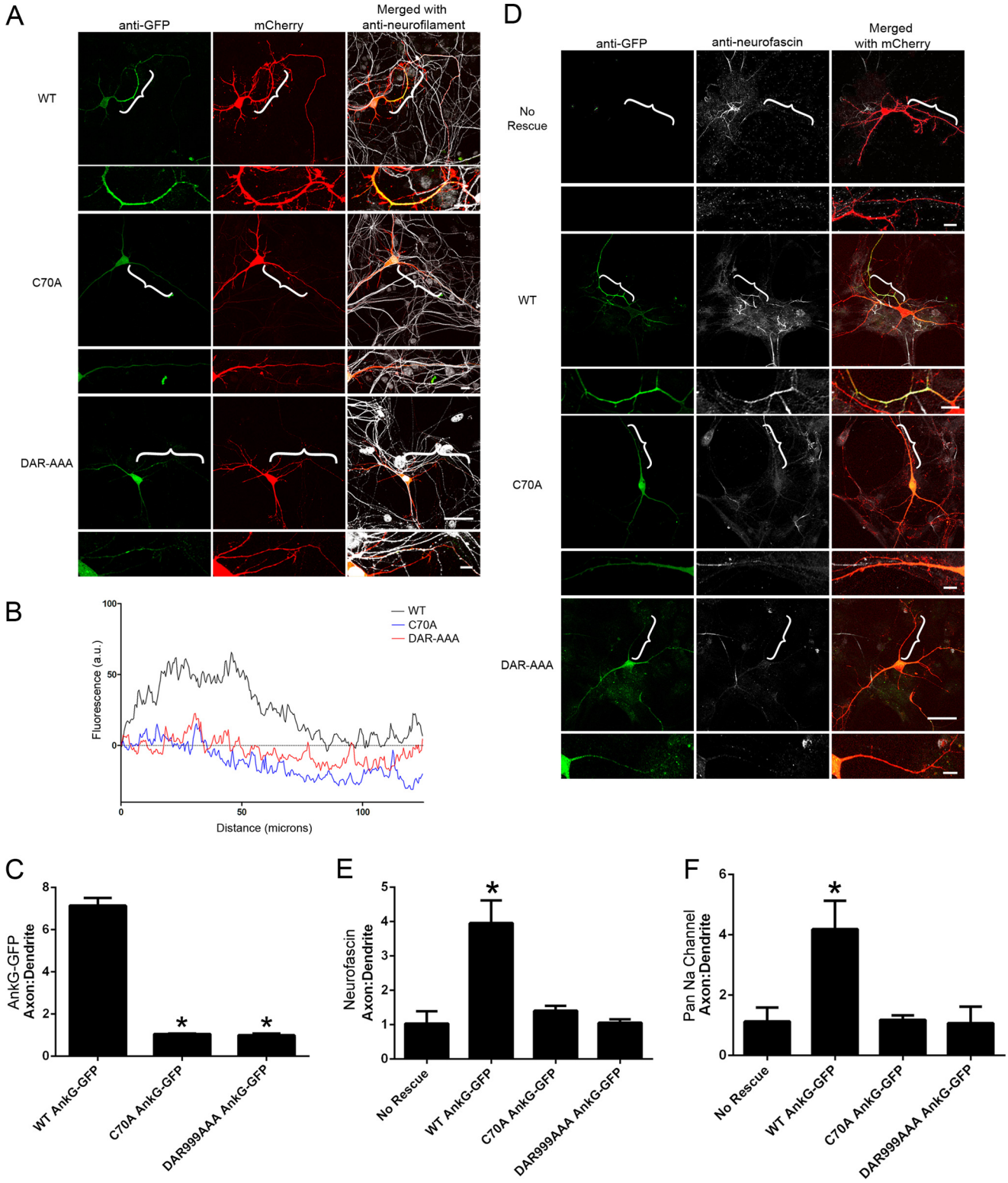

to exclude the possibility that the partial recovery is an artifact resulting from total fluorescence loss, we analyzed our data by normalizing to an unbleached region (for details, see "Experimental Procedures"). We found that C70A mutation showed no significant increase in the mobile fraction or the initial rate of AnkG recovery within 5 min (Fig. 6, *A* and *B*). However, loss of β_2-spectrin interaction through the DAR999AAA mutation further increased the mobile fraction by more than 30%, indicating that AnkG is restricted by association with β_2-spectrin (Fig. 6, *A* and *B*). The double mutant C70A/DAR999AAA AnkG showed no further increase in recovery compared with DAR999AAA mutation alone (Fig. 6, *A* and *B*). These FRAP data demonstrate that a substantial fraction of lateral membrane-associated AnkG is immobile over a 5-min measurement and that loss of interaction with β_2-spectrin but not C70A mutation increases the mobile fraction of AnkG.

C70A Mutation Abolishes AnkG Function in Lateral Membrane Biosynthesis—AnkG collaborates with β_2-spectrin in biogenesis of the lateral membrane in human bronchial epithelial cells (8, 18). We evaluated effects of the C70A mutation on this AnkG function by knocking down endogenous AnkG in MDCK cells followed by rescue with GFP-tagged wild-type or mutant AnkG. We generated a doxycycline-inducible AnkG shRNA MDCK stable cell line with a hairpin sequence targeting the ankyrin repeat domain. The targeting vector included the fluorescent protein mCherry, which allowed isolation of infected cells by FACS. RT-PCR (data not shown) and immunoblotting showed that 48-h induction by doxycycline diminished 210-kDa AnkG by more than 90% at both mRNA and protein levels without affecting the 100- and 120-kDa isoforms (Fig. 7*A*). We observed that when AnkG is silenced by 90%, lateral membrane height is reduced from 10 to 3 μm (Fig. 7, *B* and *C*) (8). When cells depleted of endogenous AnkG were transfected with WT 190-kDa AnkG-GFP, the lateral membrane was restored to its normal height, as reported previously (8). However, expression of C70A 190-kDa AnkG failed to rescue lateral membrane height and resulted in further intracellular accumulation of AnkG-GFP (Fig. 7*B*). Of note, we found that rescue of lateral membrane height was dependent on expression of the rescue plasmid in adjacent cells, because cells that shared a cell-cell contact with a non-transfected cell demonstrated much lower cell heights.

C70A Mutation Abolishes Function of 270-kDa AnkG at the Axon Initial Segment—270/480-kDa AnkG concentrates at the AIS of neurons throughout the peripheral and central nervous system and recruits β_4-spectrin and neurofascin (2, 3, 37). None of the known binding partners for AnkG are sufficient for its localization to the AIS (5, 14). We determined whether Cys-70 plays a role in targeting of 270-kDa AnkG to the AIS of cultured hippocampal neurons using a similar knockdown and replacement strategy as used in MDCK cells. By transfecting cells at 4–5 days *in vitro*, we are able to rescue AnkG expression during AIS formation to test the function of the mutant proteins. C70A 270-kDa AnkG-GFP concentrated normally at the AIS in hippocampal neurons containing endogenous AnkG and intact AIS (supplemental Fig. S1). However, if endogenous AnkG was depleted by shRNA, C70A AnkG was unable to cluster at the AIS region and instead distributed evenly in the soma, dendrites, and axon of transfected neurons (Fig. 8, *A* and *B*). Similarly, interaction with spectrin is also critical for formation of the initial segment, because DAR999AAA was also unable to cluster at the AIS (Fig. 8, *A* and *B*). Moreover, C70A 270-kDa AnkG also lost the ability to cluster neurofascin and voltage-gated sodium channels to the AIS (Fig. 8, *D–F*, and supplemental Fig. S2). This loss of the ability to recruit neurofascin to the AIS is not a result of a loss of neurofascin binding because the AnkG double mutant (C70A/DAR999AAA) still interacts with neurofascin in the membrane recruitment assay in 293 cells (Fig. 5). These results are consistent with a requirement for palmitoylation for function of AnkG at the AIS as well as epithelial lateral membranes.

DISCUSSION

Here we demonstrate that AnkG is *S*-palmitoylated at cysteine 70 in MDCK cells and that the C70A mutation abolishes the activity of AnkG in biogenesis of epithelial lateral membranes and assembly of the AIS in neurons. We also find that C70A mutation prevents association of AnkG with the plasma membrane of unpolarized MDCK cells. The C70A mutation is unlikely to result in loss of folding of AnkG because this residue is located in a predicted solvent-exposed loop of an ankyrin repeat (Fig. 3*A*). Moreover, the C70A mutation has no effect on interaction of AnkG with polarized MDCK cell lateral membranes or on interaction with E-cadherin or neurofascin. The effects of C70A mutation are therefore consistent with a requirement of *S*-palmitoylation for function of AnkG at epithelial lateral membranes and the AIS. However, it is important to note that we cannot exclude other interpretations, such as requirement of cysteine 70 for interaction with unidentified proteins.

A critical step in developing the palmitoylation hypothesis will be to identify which of the 24 palmitoyltransferases are

FIGURE 8. **C70A mutation abolishes 270-kDa AnkG clustering and function at axon initial segments in hippocampal neurons.** Neonatal mouse-derived hippocampal neurons were grown in tissue culture for 4–5 days following a standard protocol. Cells in MatTek plates were co-transfected with 500 ng of AnkG shRNA plasmids and 500 ng of wild type, C70A, or DAR999AAA 270-kDa AnkG-GFP plasmids or just 500 ng of AnkG shRNA plasmid alone (*No Rescue*). Two days after transfection, cells were fixed with 4% PFA in PBS buffer at room temperature for 15 min, permeabilized by methanol at −20 °C for 7 min, and processed for immunofluorescence. *A*, anti-GFP staining for 270-kDa AnkG-GFP shown in *green*, mCherry marking transfected neurons shown in *red*, and the axonal marker neurofilament shown in *white* (*scale bar*, 50 μm). *Brackets* mark the axon initial segment, which is shown at higher magnification *below* each image (*scale bar*, 10 μm). *B*, quantification of fluorescence intensity along the axons. The immunofluorescence intensity in the soma was normalized to 1. Average data from 10 neurons per condition are shown. *C*, quantification of the anti-GFP fluorescence intensity ratio of axons to dendrites in cells depleted of endogenous 270-kDa AnkG and rescued with WT, C70A, or DAR999AAA AnkG-GFP ($n = 3$; *, $p < 0.05$). *D*, anti-GFP staining for 270-kDa AnkG-GFP shown in *green*, anti-neurofascin staining shown in *white*, and mCherry marking transfected neurons shown in *red*. Axons were identified by morphology (*scale bar*, 50 μm). *Brackets* mark the axon initial segment, which is shown at higher magnification *below* each *image* (*scale bar*, 10 μm). *E*, quantification of the anti-endogenous neurofascin fluorescence intensity ratio of axons to dendrites in cells depleted of endogenous 270-kDa AnkG and rescued with mock (*No Rescue*), WT, C70A, or DAR999AAA AnkG-GFP ($n = 3–4$; *, $p < 0.05$). *F*, quantification of the anti-endogenous pan-sodium channel fluorescence intensity ratio of axons to dendrites in cells depleted of endogenous 270-kDa AnkG and rescued with mock (*No Rescue*), WT, C70A, or DAR999AAA AnkG-GFP ($n = 5$; *, $p < 0.05$). *Error bars*, S.E.

responsible for modification of AnkG. These enzymes exhibit specific expression and localization patterns and determine protein subcellular targeting, protein stability, and membrane micropatterning (38, 39). Cys-70 is conserved among three ankyrin isoforms and across vertebrate species as well as one of the *Drosophila* ankyrin genes (Fig. 3*B*). Therefore, it also will be important to evaluate palmitoylation of other ankyrin members and to determine if there is a conserved palmitoylation-dependent targeting mechanism shared by the ankyrin family.

FRAP measurements of WT AnkG-GFP motility on the lateral membrane in MDCK cells surprisingly show a limited mobile fraction, which can be increased by 30% upon loss of β_2-spectrin interaction but not by loss of palmitoylation (Fig. 6, *A* and *B*). The increased recovery with loss of spectrin binding is unlikely to result from plasma membrane-cytoplasm protein exchange, because WT AnkG-GFP reaches a steady plateau at only 40% fractional recovery. Our findings, for the first time, suggest the existence of membrane subdomains or compartments, which may coordinate AnkG, β_2-spectrin, and possibly other proteins. These proposed domains could play important roles in limiting AnkG dynamics on the lateral membrane. Although the C70A mutation shows no effect on AnkG mobility, palmitoylation could be involved in organizing membrane subdomains. Interestingly, it has been reported that palmitoylated proteins are targeted to "lipid rafts" (40–42). Furthermore, neurofascin, an AnkG binding partner, is palmitoylated at a site in the transmembrane domain conserved among the L1CAM family (43). It will be of interest to study how the doubly palmitoylated AnkG-neurofascin complexes alter properties of membrane domains in neurons. It also will be important in future experiments to directly visualize the distribution of AnkG and other palmitoylated proteins at those membrane domains using high resolution three-dimensional microscopy.

A striking finding that stimulated our discovery of *S*-palmitoylation of AnkG was the retention of AnkG at the plasma membrane of unpolarized MDCK cells grown in low calcium (Fig. 1*A*). AnkG is the only lateral membrane-associated protein that we are aware of that persists under low calcium conditions, and this behavior depends on Cys-70 (Fig. 4, *A* and *B*). Residual AnkG is not associated with its partners β_2-spectrin and E-cadherin, which are located in the cytoplasm. AnkG thus may function as a template during reassembly of these proteins on the lateral membrane following restoration of calcium. It is tempting to speculate that residual AnkG remains membrane-associated through its Cys-70 palmitate modification. In this case, lipid-based patterning of AnkG and other palmitoylated proteins may play important roles in determining lateral membrane identity.

Acknowledgments—We thank the Duke Proteomics Core Facility for mass spectrometry data analysis and the Duke Flow Cytometry Facility for cell sorting to establish the inducible AnkG shRNA cell line.

REFERENCES

1. Bennett, V., and Healy, J. (2008) Organizing the fluid membrane bilayer. Diseases linked to spectrin and ankyrin. *Trends Mol. Med.* **14,** 28–36
2. Jenkins, S. M., and Bennett, V. (2001) Ankyrin-G coordinates assembly of the spectrin-based membrane skeleton, voltage-gated sodium channels, and L1 CAMs at Purkinje neuron initial segments. *J. Cell Biol.* **155,** 739–746
3. Zhou, D., Lambert, S., Malen, P. L., Carpenter, S., Boland, L. M., and Bennett, V. (1998) AnkyrinG is required for clustering of voltage-gated Na channels at axon initial segments and for normal action potential firing. *J. Cell Biol.* **143,** 1295–1304
4. Pan, Z., Kao, T., Horvath, Z., Lemos, J., Sul, J. Y., Cranstoun, S. D., Bennett, V., Scherer, S. S., and Cooper, E. C. (2006) A common ankyrin-G-based mechanism retains KCNQ and NaV channels at electrically active domains of the axon. *J. Neurosci.* **26,** 2599–2613
5. Hedstrom, K. L., Xu, X., Ogawa, Y., Frischknecht, R., Seidenbecher, C. I., Shrager, P., and Rasband, M. N. (2007) Neurofascin assembles a specialized extracellular matrix at the axon initial segment. *J. Cell Biol.* **178,** 875–886
6. Hedstrom, K. L., Ogawa, Y., and Rasband, M. N. (2008) AnkyrinG is required for maintenance of the axon initial segment and neuronal polarity. *J. Cell Biol.* **183,** 635–640
7. Sobotzik, J. M., Sie, J. M., Politi, C., Del Turco, D., Bennett, V., Deller, T., and Schultz, C. (2009) AnkyrinG is required to maintain axo-dendritic polarity *in vivo*. *Proc. Natl. Acad. Sci. U.S.A.* **106,** 17564–17569
8. Kizhatil, K., and Bennett, V. (2004) Lateral membrane biogenesis in human bronchial epithelial cells requires 190-kDa ankyrin-G. *J. Biol. Chem.* **279,** 16706–16714
9. Kizhatil, K., Baker, S. A., Arshavsky, V. Y., and Bennett, V. (2009) Ankyrin-G promotes cyclic nucleotide-gated channel transport to rod photoreceptor sensory cilia. *Science* **323,** 1614–1617
10. Ayalon, G., Davis, J. Q., Scotland, P. B., and Bennett, V. (2008) An ankyrin-based mechanism for functional organization of dystrophin and dystroglycan. *Cell* **135,** 1189–1200
11. Lowe, J. S., Palygin, O., Bhasin, N., Hund, T. J., Boyden, P. A., Shibata, E., Anderson, M. E., and Mohler, P. J. (2008) Voltage-gated Nav channel targeting in the heart requires an ankyrin-G dependent cellular pathway. *J. Cell Biol.* **180,** 173–186
12. Mohler, P. J., Rivolta, I., Napolitano, C., LeMaillet, G., Lambert, S., Priori, S. G., and Bennett, V. (2004) Nav1.5 E1053K mutation causing Brugada syndrome blocks binding to ankyrin-G and expression of Nav1.5 on the surface of cardiomyocytes. *Proc. Natl. Acad. Sci. U.S.A.* **101,** 17533–17538
13. Hund, T. J., Koval, O. M., Li, J., Wright, P. J., Qian, L., Snyder, J. S., Gudmundsson, H., Kline, C. F., Davidson, N. P., Cardona, N., Rasband, M. N., Anderson, M. E., and Mohler, P. J. (2010) A β(IV)-spectrin/CaMKII signaling complex is essential for membrane excitability in mice. *J. Clin. Invest.* **120,** 3508–3519
14. Zhang, X., and Bennett, V. (1998) Restriction of 480/270-kD ankyrin G to axon proximal segments requires multiple ankyrin G-specific domains. *J. Cell Biol.* **142,** 1571–1581
15. Boiko, T., Vakulenko, M., Ewers, H., Yap, C. C., Norden, C., and Winckler, B. (2007) Ankyrin-dependent and -independent mechanisms orchestrate axonal compartmentalization of L1 family members neurofascin and L1/neuron-glia cell adhesion molecule. *J. Neurosci.* **27,** 590–603
16. Dzhashiashvili, Y., Zhang, Y., Galinska, J., Lam, I., Grumet, M., and Salzer, J. L. (2007) Nodes of Ranvier and axon initial segments are ankyrin G-dependent domains that assemble by distinct mechanisms. *J. Cell Biol.* **177,** 857–870
17. Galiano, M. R., Jha, S., Ho, T. S., Zhang, C., Ogawa, Y., Chang, K. J., Stankewich, M. C., Mohler, P. J., and Rasband, M. N. (2012) A distal axonal cytoskeleton forms an intra-axonal boundary that controls axon initial segment assembly. *Cell* **149,** 1125–1139
18. Kizhatil, K., Yoon, W., Mohler, P. J., Davis, L. H., Hoffman, J. A., and Bennett, V. (2007) Ankyrin-G and β_2-spectrin collaborate in biogenesis of lateral membrane of human bronchial epithelial cells. *J. Biol. Chem.* **282,** 2029–2037
19. Levental, I., Grzybek, M., and Simons, K. (2010) Greasing their way. Lipid modifications determine protein association with membrane rafts. *Biochemistry* **49,** 6305–6316
20. Bennett, V., and Stenbuck, P. J. (1980) Human erythrocyte ankyrin. Purification and properties. *J. Biol. Chem.* **255,** 2540–2548
21. Staufenbiel, M. (1987) Ankyrin-bound fatty acid turns over rapidly at the erythrocyte plasma membrane. *Mol. Cell Biol.* **7,** 2981–2984

22. Drisdel, R. C., Alexander, J. K., Sayeed, A., and Green, W. N. (2006) Assays of protein palmitoylation. *Methods* **40,** 127–134
23. Martinez-Palomo, A., Meza, I., Beaty, G., and Cereijido, M. (1980) Experimental modulation of occluding junctions in a cultured transporting epithelium. *J. Cell Biol.* **87,** 736–745
24. Siliciano, J. D., and Goodenough, D. A. (1988) Localization of the tight junction protein, ZO-1, is modulated by extracellular calcium and cell-cell contact in Madin-Darby canine kidney epithelial cells. *J. Cell Biol.* **107,** 2389–2399
25. Mattey, D. L., and Garrod, D. R. (1986) Calcium-induced desmosome formation in cultured kidney epithelial cells. *J. Cell Sci.* **85,** 95–111
26. Gumbiner, B., Stevenson, B., and Grimaldi, A. (1988) The role of the cell adhesion molecule uvomorulin in the formation and maintenance of the epithelial junctional complex. *J. Cell Biol.* **107,** 1575–1587
27. Kaiser, H. W., O'Keefe, E., and Bennett, V. (1989) Adducin. Ca^{2+}-dependent association with sites of cell-cell contact. *J. Cell Biol.* **109,** 557–569
28. Busche, S., Kremmer, E., and Posern, G. (2010) E-cadherin regulates MAL-SRF-mediated transcription in epithelial cells. *J. Cell Sci.* **123,** 2803–2809
29. Nelson, W. J., and Veshnock, P. J. (1987) Ankyrin binding to (Na^+ + K^+)ATPase and implications for the organization of membrane domains in polarized cells. *Nature* **328,** 533–536
30. Salaun, C., Greaves, J., and Chamberlain, L. H. (2010) The intracellular dynamic of protein palmitoylation. *J. Cell Biol.* **191,** 1229–1238
31. Staufenbiel, M. (1988) Fatty acids covalently bound to erythrocyte proteins undergo a differential turnover *in vivo*. *J. Biol. Chem.* **263,** 13615–13622
32. Peters, L. L., John, K. M., Lu, F. M., Eicher, E. M., Higgins, A., Yialamas, M., Turtzo, L. C., Otsuka, A. J., and Lux, S. E. (1995) Ank3 (epithelial ankyrin), a widely distributed new member of the ankyrin gene family and the major ankyrin in kidney, is expressed in alternatively spliced forms, including forms that lack the repeat domain. *J. Cell Biol.* **130,** 313–330
33. Forrester, M. T., Hess, D. T., Thompson, J. W., Hultman, R., Moseley, M. A., Stamler, J. S., and Casey, P. J. (2011) Site-specific analysis of protein S-acylation by resin-assisted capture. *J. Lipid Res.* **52,** 393–398
34. Jennings, B. C., and Linder, M. E. (2012) DHHC protein *S*-acyltransferases use similar ping-pong kinetic mechanisms but display different acyl-CoA specificities. *J. Biol. Chem.* **287,** 7236–7245
35. Kizhatil, K., Davis, J. Q., Davis, L., Hoffman, J., Hogan, B. L., and Bennett, V. (2007) Ankyrin-G is a molecular partner of E-cadherin in epithelial cells and early embryos. *J. Biol. Chem.* **282,** 26552–26561
36. Henis, Y. I., Rotblat, B., and Kloog, Y. (2006) FRAP beam-size analysis to measure palmitoylation-dependent membrane association dynamics and microdomain partitioning of Ras proteins. *Methods* **40,** 183–190
37. Kordeli, E., Lambert, S., and Bennett, V. (1995) AnkyrinG. A new ankyrin gene with neural-specific isoforms localized at the axonal initial segment and node of Ranvier. *J. Biol. Chem.* **270,** 2352–2359
38. Greaves, J., and Chamberlain, L. H. (2010) *S*-acylation by the DHHC protein family. *Biochem. Soc. Trans.* **38,** 522–524
39. Aicart-Ramos, C., Valero, R. A., and Rodriguez-Crespo, I. (2011) Protein palmitoylation and subcellular trafficking. *Biochim. Biophys. Acta* **1808,** 2981–2994
40. Delint-Ramirez, I., Willoughby, D., Hammond, G. V., Ayling, L. J., and Cooper, D. M. (2011) Palmitoylation targets AKAP79 protein to lipid rafts and promotes its regulation of calcium-sensitive adenylyl cyclase type 8. *J. Biol. Chem.* **286,** 32962–32975
41. Linder, M. E., and Deschenes, R. J. (2007) Palmitoylation. Policing protein stability and traffic. *Nat. Rev. Mol. Cell Biol.* **8,** 74–84
42. Fragoso, R., Ren, D., Zhang, X., Su, M. W., Burakoff, S. J., and Jin, Y. J. (2003) Lipid raft distribution of CD4 depends on its palmitoylation and association with Lck and evidence for CD4-induced lipid raft aggregation as an additional mechanism to enhance CD3 signaling. *J. Immunol.* **170,** 913–921
43. Ren, Q., and Bennett, V. (1998) Palmitoylation of neurofascin at a site in the membrane-spanning domain highly conserved among the L1 family of cell adhesion molecules. *J. Neurochem.* **70,** 1839–1849